17. J. Ryuta, T. Yoshimi, H. Kondo, H. Okuda, and Y. Shimanuki, *Jpn. J. Appl. Phys.*, **31**, 2338 (1992).
18. Y. Mori and K. Venura, *This Journal*, **142**, 3104 (1995).
19. J. P. Joly, in *Crystalline Defects and Contamination: Their Impact and Control in Device Manufacturing II*, B. O. Kolbesen, P. Stallhofer, C. Claeys, and F. Tardiff, Editors, PV 97-22, p. 259, The Electrochemical Society Proceedings Series, Pennington, NJ (1997).

# Radio-Frequency Reactively Sputtered $VO_x$ Thin Films Deposited at Different Oxygen Flows

**A. Lourenço and A. Gorenstein***

*DFA/IFGW/UNICAMP, CEP 13084-970 Campinas, SP, Brazil*

**S. Passerini* and W. H. Smyrl***

*Corrosion Research Center, Chemical Engineering and Material Science, University of Minnesota, Minneapolis, Minnesota 55455, USA*

**M. C. A. Fantini and M. H. Tabacniks**

*Instituto de Fisica-USP, CEP 05389-970 São Paulo, SP, Brazil*

ABSTRACT

The effect of different oxygen flow rate on the properties of vanadium oxide thin films formed by radio-frequency, reactive sputtering deposition are investigated. The stoichiometry of the as-deposited films was investigated by Rutherford backscattering spectrometry. For high oxygen flows, films were mainly $V_2O_5$ while a lower oxide was obtained at the lowest flow. Forward recoil spectrometry indicated a significant hydrogen content in the thin films. X-ray diffraction showed that the films were amorphous. The electrochromism shown by such films upon lithium intercalation was also studied. Samples deposited at high oxygen flow were transparent/yellow, and showed a somewhat complicated electrochromic behavior. Upon lithium insertion up to 25 mC/cm$^2$, the films acted as cathodically coloring materials at wavelengths higher than 500 nm and as anodically coloring material at lower wavelengths. For the higher insertion levels, the opposite behavior was observed. Samples deposited at very low $O_2$ flows showed no electrochromic behavior.

## Introduction

Electrochromic materials[1] are usually classified as anodically or cathodically coloring materials, depending on the direction of color change upon ion intercalation. Although such a classification is sometime misleading, it is commonly used. Nickel oxide[2] is a well-known example of an anodically coloring material in aqueous electrolyte while tungsten trioxide[3] is the ideal cathodically coloring material either in aqueous or aprotic electrolytes. Vanadium pentoxide,[4] however, presents a different behavior. In the beginning of the intercalation process (low intercalant concentration), it behaves as a cathodically coloring material, for some wavelengths and till a certain intercalation level; from this point on, the reverse behavior is observed. This behavior has been interpreted in terms of the band structure of $V_2O_5$,[5] and is discussed below. As a consequence, transmittance changes are limited in these materials. $V_2O_5$ has been proposed as an adequate optically passive counter electrode in rocking-chair electrochromic devices.[6] Lower vanadium oxides, such as $V_6O_{13}$ and $VO_2$ are also interesting intercalation compounds with promising behavior in the fields of rechargeable lithium batteries[7] and chromogenic devices.[1]

Thin films of vanadium oxides can be obtained by different techniques. As usually observed in thin film deposition, the films have microstructures and compositions that are markedly dependent on the growth technique and deposition parameters. The different deposition methods and film characteristics for vanadium oxides have been recently reviewed.[1]

In the present work, we investigated the effect of oxygen content in the O/Ar plasma during the deposition of vanadium oxide films by radio frequency (rf) reactive sputtering. The composition of the as grown samples was investigated by Rutherford backscattering spectrometry (RBS) and forward recoil spectrometry (FRS). The microstructure was investigated by X-ray diffraction. The electrochromism observed in these materials upon lithium intercalation was also investigated.

## Experimental

Vanadium oxide thin films were deposited by rf reactive sputtering on ITO-coated thick glass plates. The substrates were located at 12 cm from the metallic vanadium target. The rf power was 200 W. The pressure in the sputtering chamber before deposition was $1.5 \times 10^{-6}$ mTorr. During deposition, the pressure (Ar + $O_2$) was maintained at a constant level ($7.0 \times 10^{-3}$ mTorr), while the $O_2$ flow was varied in the range 1.00 to 9.00 scc/min. The thicknesses of the deposited films were measured by profilometry and are reported in Table I.

The X-ray diffraction (XRD) measurements were performed using Ni filter Cu Kα radiation.

RBS and FRS analyses were performed at the IBM Almaden Research Center, San Jose, California, using a 3 MeV NEC Pelletron accelerator. RBS experiments were performed by using a 2.3 MeV $He^+$ beam, with scattering angle of 170°. FRS measurements were used for H analysis with a target tilt angle of 75° and a 30° detection angle. A

**Table I. Thicknesses of the as-deposited films and mean composition.**

| $O_2$ flow sccm | Thickness, nm | Mean composition |
|---|---|---|
| 1.00 | 250 | $VO_{2.4}H_{0.44}$ |
| 1.25 | 250 | $VO_{2.79}H_{0.96}$ |
| 1.50 | 200 | $VO_{2.83}H_{0.96}$ |
| 3.00 | 200 | $VO_{2.78}H_{0.91}$ |
| 9.00 | 185 | $VO_{2.62}H_{0.95}$ |

* Electrochemical Society Active Member.

7 μm thick Al absorber was used to filter the recoiled He from the scattered beam.

Electrochemical lithium intercalation experiments were pursued by placing the samples in a three-electrode, one-compartment cell in which 1 M $LiClO_4$/propylene carbonate was used as electrolyte. A lithium foil was used as the counter electrode and a metallic Ag strip was used as pseudo-reference electrode (2.72 V vs Li, in this electrolyte). The electrodes were mounted in a sealed Teflon electrochemical cell with two parallel optical windows. The cell assembly was done in an argon-filled dry box with a water content below 1 ppm. Monochromatic transmittance or spectral transmittance were measured in situ by using a He-Ne laser ($\lambda$ = 632.8 nm) or a double-beam Lambda 9 Perkin-Elmer spectrophotometer, respectively. These measurements were made with the sample imersed in the electrolyte, by aligning the optical windows of the electrochemical cell with the optical beam. Potentiodynamic experiments were performed using a 273 EG&G potentiostat/galvanostat.

## Results and Discussion

*As-deposited films: optical properties, microstructure, and composition.*—Figure 1 presents the deposition rate as a function of oxygen flow ($\phi$) during deposition. The deposition rate was calculated by dividing the thickness of each sample by the deposition time. For comparison purposes, data obtained for deposition in similar conditions but using other metallic targets (Ni or Mo) are also shown. The curves in Fig. 1 show an initial increase in the deposition rate, followed by a decrease with increasing $\phi$. The latter effect is associated with the oxidation of the metallic target and it is much more effective for the vanadium target than for the other materials. Aita and co-workers,[8-10] have discussed extensively the mechanism of reactive sputtering for vanadium oxide films. They noted that below a critical value of the $O_2$ content in the deposition chamber, the plasma containing neutral vanadium atoms. Above this critical value, no more metallic vanadium atoms are detected, and vanadium is transferred from the oxidized target to the substrate in molecular form, i.e., bonded to oxygen.[9] Therefore, it can be expected that films deposited at a higher $\phi$ than the critical value, should have similar compositions. The critical value for the samples in this work is around $\phi$ = 1.5–2 sccm, where an abrupt reduction of the deposition rate (Fig. 1) is observed.

XRD measurements performed on all samples did not show any diffraction peak. The films were either amorphous or small-grained materials (less than 5 nm).

Figure 2 shows optical transmittance data for the as-grown samples. Samples deposited at $\phi$ of 1 and 1.25 sccm were gray. All the other samples had the characteristic yellow color of $V_2O_5$.

From the transmittance and reflectance data (not shown), the absorption coefficients were calculated. According to the Tauc model for amorphous semiconductors,[11] an indirect band to band transition should give a linear relationship in a $(\alpha h\nu)^{1/2}$ vs $h\nu$ plot (not shown). An extrapolation toward zero absorption gives the optical gap, $E_{opt}$. These results are shown in Fig. 3. The highest $E_{opt}$ value is obtained for the sample grown at low $\phi$ ($E_{opt}$ = 2.56 eV, $\phi$ = 1 sccm). For higher $\phi$, $E_{opt}$ is in the range 2.41–2.45 eV. Data in the literature for rf sputtered vanadium pentoxide films are in the range 2.15–2.4 eV, [5,10,12] i.e., in good agreement with the present results.

In Fig. 4a are reported the results obtained from RBS and FRS measurements, in terms of oxygen/vanadium ([O/V]) and hydrogen/vanadium [H/V]) ratios in the thin films. The [H/V] ratio is lower than 1 only for the lowest $\phi$ (1 sccm). Higher hydrogen content is found for the higher flow rate. The mean overall composition of such film, calculated from these data, is shown in Table I.

From the thin film composition and assuming that the hydrogen formed only O-H bonds, the mean valence of vanadium in the sputtered samples can be calculated. The results are illustrated in Fig. 4b. For comparison purposes, the two lines corresponding to the mean oxidation state of vanadium in $V_6O_{13}$ (4.33) and in $V_2O_5$ (5.0), are also drawn in the figure. Surprisingly, the sample prepared at the highest $\phi$ shows the lowest mean oxidation state. Such a

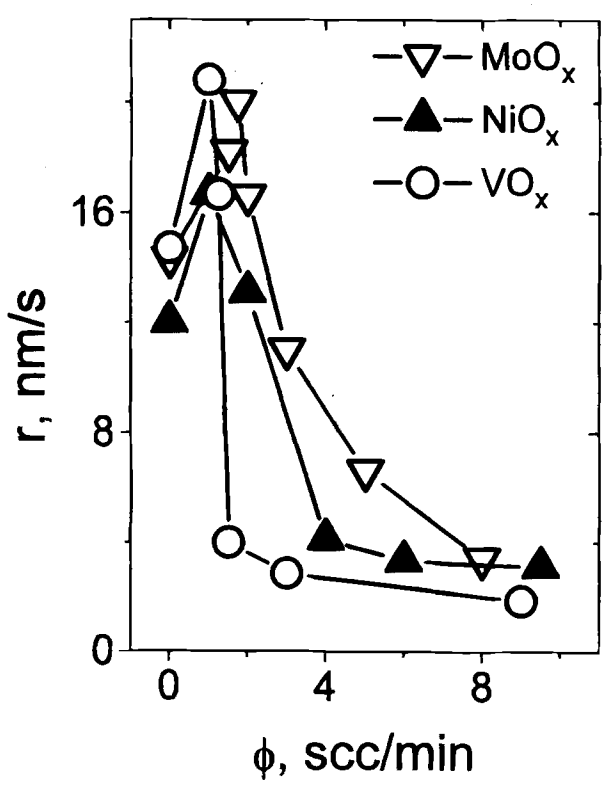


Fig. 1. Deposition rate as a function of $O_2$ flow during deposition shown by different metallic targets (Ni, Mo, or V).

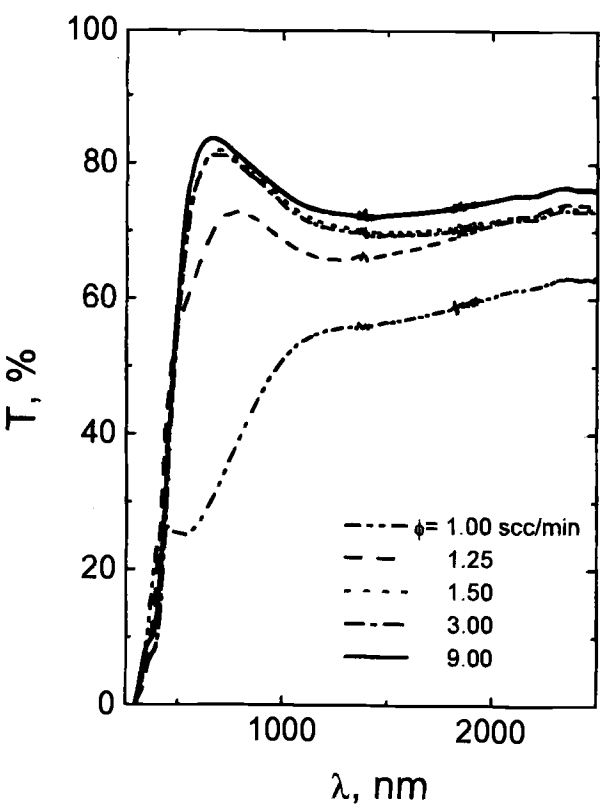


Fig. 2. Spectral transmittance of thin film vanadium oxide samples deposited with different oxygen flows.

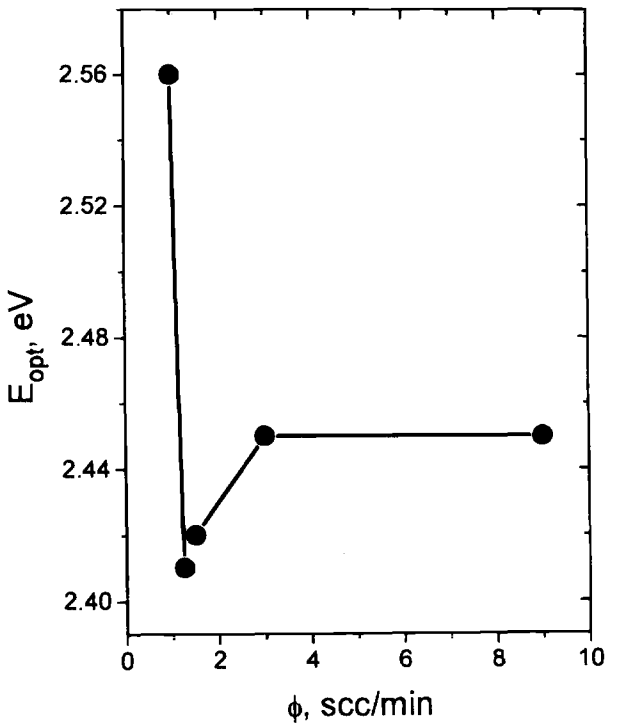


**Fig. 3. Optical gap of thin film vanadium oxide samples as a function of $O_2$ flow during deposition.**

result is in contrast with the optical characterization. In fact, the films deposited at $\phi < 1.5$ sccm were gray and this color is characteristic of lower vanadium oxides like $VO_2$ and $V_6O_{13}$. On the contrary, the films prepared with $\phi > 1.5$ sccm had the characteristic yellow color of $V_2O_5$. Such indications were also confirmed by XPS analysis[13] that has shown the contemporaneous presence of vanadium at both low and high oxidation states in the samples prepared at lower $\phi$.

Such a contradiction clearly indicate that the previous assumption regarding the formation of O-H bonds is not valid. The films deposited at $\phi > 1.5$ sccm are mainly $V_2O_5$ in accordance with the optical gap values and XPS results. The hydrogen in the films is certainly bonded to oxygen not only to form O-H groups but also water molecules with a ratio that depends on several factors like deposition time and rate, film morphology and crystallinity, sputtering chamber degassing or exposition of the sample to humid atmosphere. It is not clear yet if film hydration occurred during the deposition or after exposure to the atmosphere. However, hydrogen was also detected in other materials deposited by rf sputtering in similar conditions.[14]

Summarizing, the rf sputtered vanadium oxide films were amorphous with a high hydrogen content, bonded to oxygen to form O-H groups or water molecules. The main valence of the films deposited at high $\phi$ was 5+, compatible with the $V_2O_5$ stoichiometry. Lower valence oxides were deposited at low $\phi$.

*Intercalation and electrochromism.*—As discussed in the experimental section, the electrochromic properties of the films were investigated by intercalating $Li^+/e^-$ into the oxide matrix. Figure 5a presents the potentiodynamic profile for three samples deposited at a $\phi$ of 1, 1.5, and 9 sccm, respectively. Figure 5b presents the associated monochro-

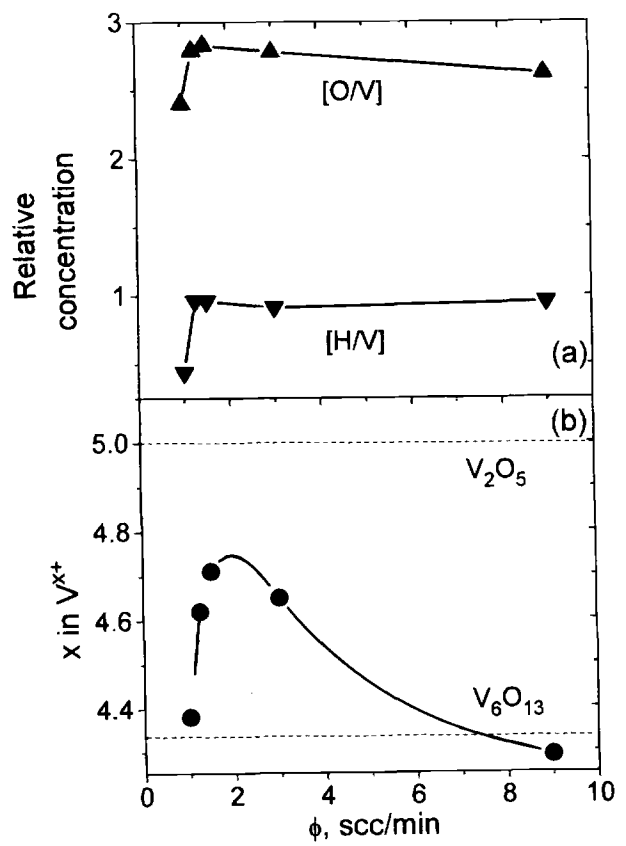


**Fig. 4. (a) [H/V] and [O/V] ratios in thin film vanadium oxide samples as a function of $O_2$ flow during deposition; (b) mean valence of vanadium ions.**

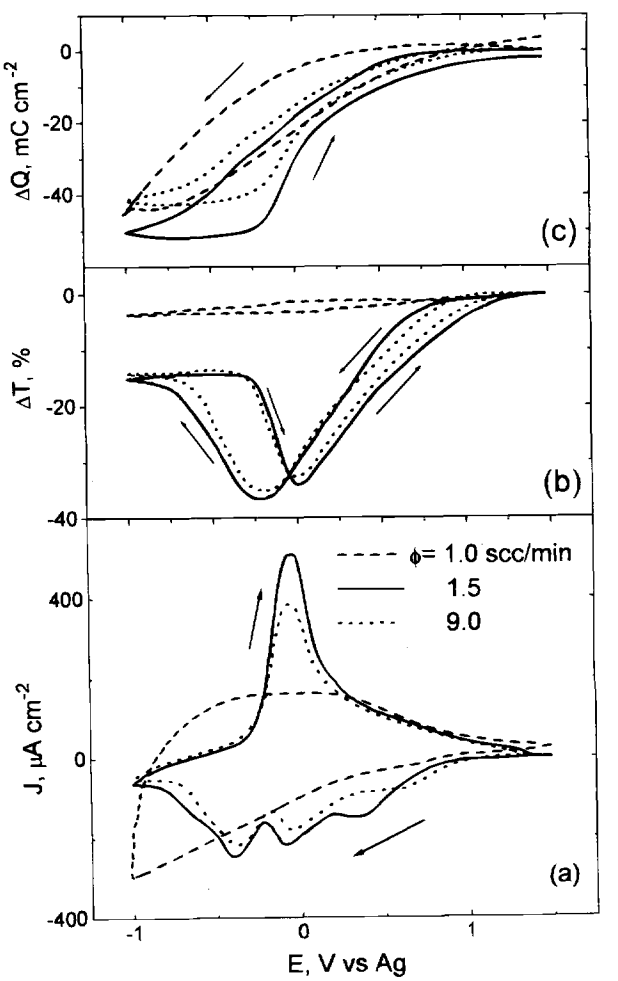


**Fig. 5. Potentiodynamic experiments on thin film vanadium oxide samples deposited with different oxygen flows. (a) I-V plot and associated (b) monochromatic transmittance ($\lambda$ = 632.8 nm) and (c) charge changes. Scan rate: 5 mV/s.**

matic transmittance changes, and Fig. 5c the charge density variation.

The potentiodynamic profile, transmittance, and charge variations for samples deposited at a $\phi$ of 1.5 and 9.0 sccm were very similar. Three distinct cathodic peaks were clearly shown by these samples, at −0.4, −0.1, and 0.33 V vs Ag (2.32, 2.62, and 3.05 V vs Li). In crystalline $V_2O_5$ materials, these peaks have been associated with the well-known progressive crystallographic phase transitions showed by $Li_xV_2O_5$ with increasing $x$.[15,16] Quasi-equilibrium potential vs composition plots present a sequence of constant potential regions separated by abrupt potential changes. The potential plateaus are attributed to the coexistence of two phases while the transitions are associated with a single-crystallographic phase. A different interpretation is based on the assumption that the electrochemical potential depends on the Fermi level in the material (electronic contribution) and an entropy factor (ionic contribution).[17] As a consequence, it is argued that the abrupt changes observed in the potential-composition profile maybe attributed to Fermi level jumps at defined intercalation levels.[5,18] The thin film samples discussed in this work did not show any defined diffraction peaks in the XRD patterns; they were either nanocrystalline, with small grains being undetectable by XRD, or totally amorphous. In either case, the cathodic peaks found in the thin films samples ($\phi$ = 1.5 and 9 sccm) in the potentiodynamic experiments corresponded well with other $V_2O_5$ materials either crystalline or mostly amorphous.[4] The films showed an electrochromic effect during the potentiodynamic experiment as shown by the transmittance change (at $\lambda$ = 623.8 nm) vs potential plot reported in Fig. 5b. As previously noticed by other authors,[5] the direction of the transmittance change is a function of the lithium composition. In fact, at the selected wavelength and upon a cathodic potential scan, the samples progressively darkened, acting as cathodically coloring electrodes, but then bleached as expected for anodically coloring electrodes. With the potentiodynamic conditions selected (see legend in Fig. 5), the inversion of the electrochromic behavior occurred at $x \cong 0.7$ ($x$ in $Li_xV_2O_5$) for both samples. Up to this point, the transmittance change was approximately 35% taking the initial value at 100%. At larger lithium intercalation concentrations, up to $x \cong 1.4$ and $x \cong 1.2$, respectively, for the sample deposited with a $\phi$ of 1.5 and 9 sccm, transmittance changes of about 20% were observed. The calculated electrochromic efficiencies were 8 $cm^2/C$ for both regions.

The multiple electrochromic behavior is very well demonstrated in Fig. 6 where the spectral transmittance of a sample coated at $\phi$ = 1.5 sccm is reported as a function of both wavelength and inserted charge. Upon lithium insertion of up to 25 $mC/cm^2$ ($x$ = 0.7), the film behaves as a cathodically coloring material for wavelengths larger than 480 nm and as an anodically coloring material for wavelengths lower than 480 nm. For higher intercalation levels the reverse behavior was observed.

The behavior shown by the thin films deposited at the lowest $\phi$ (1 sccm) was totally different. The potentiodynamic profile did not show any defined peak that is a characteristic of an amorphous material with coexisting multiple oxidation states.[13] Furthermore, they were electrochromically passive (Fig. 5b) in spite of their ability to intercalate lithium ions at comparable levels with the more oxidized films (Fig. 5c). Such behavior makes the lower oxidation state thin film material very promising for application as electrochromically passive electrodes.

Figure 7 presents a detail of the transmittance vs wavelength plot, at the wavelength range corresponding to the optical bandgap, $E_{opt}$. Similar to the results obtained by other researchers,[5,18] a progressive blue shift of $E_{opt}$ corresponding to a bandgap widening is clearly seen. In ref 5, this behavior has been attributed to the band structure of vanadium pentoxide. In the ionic approximation, the vanadium ions in $V_2O_5$ have the electronic configuration $4s^2\ 3d^o$ ($V^{5+}$) and the oxygen atoms have the configuration $2s^2\ 2p^6$ ($O^{2-}$). In a simplified approach, the valence band of $V_2O_5$ is mainly formed by the O 2p orbital, and the conduction band comes from the V 3d orbital. As a consequence, in the crystalline material the valence band is completely filled and the conduction band is empty. The conduction band itself is split into two subbands by the influence of the crystalline field. The lower energy band ($t_{2g}$ band) lies 0.6 eV below the main band ($e_g$ band), and can accept 6 electrons per vanadium atom in the crystal; the $e_g$ band can accept 4 electrons. Also, the $e_g$ band is larger than the $t_{2g}$ band because the V $t_{2g}$ – O 2p interactions are stronger than the V $t_{2g}$ – O 2p interactions. If a rigid band model is adopted, the filling of the bands by intercalated electrons would proceed by first completing the $t_{2g}$ band, and then the $e_g$

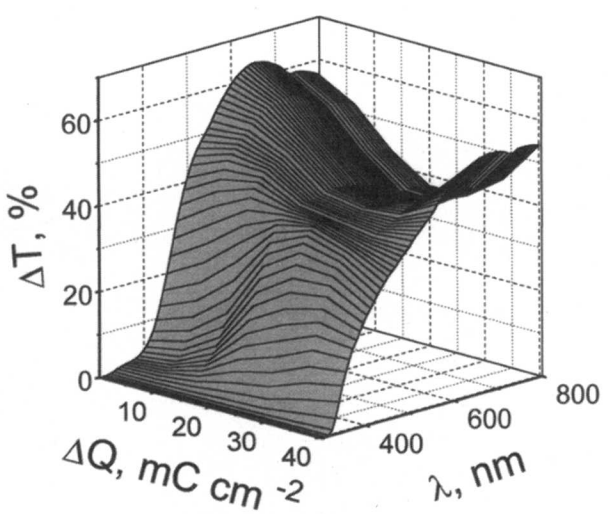


**Fig. 6. Transmittance as a function of inserted charge and wavelength. Data were obtained from consecutive potential steps. The thin film sample was deposited with $\phi$ = 1.5 sccm.**

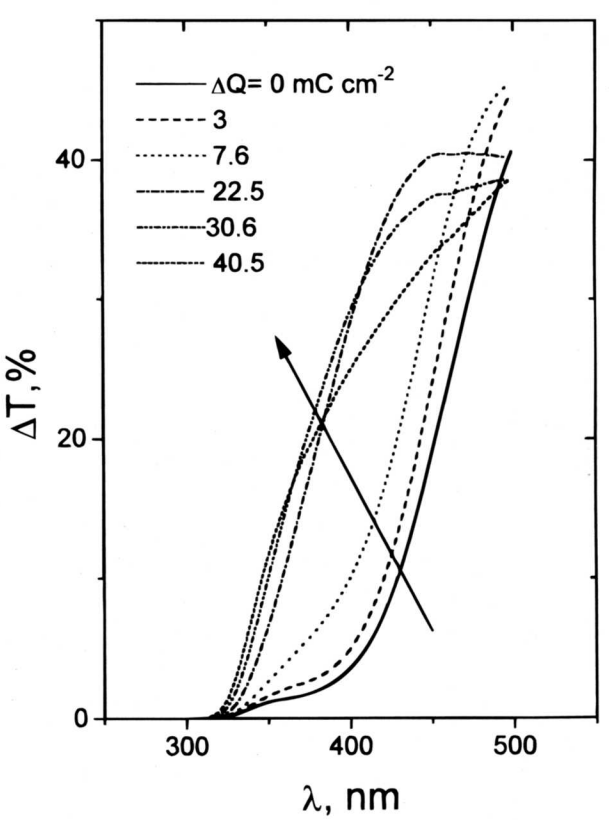


**Fig. 7. Transmittance plot in the wavelength region near the optical gap. The thin film sample was deposited at $\phi$ = 1.5 sccm.**

band, in good agreement with the detected blue shift of the optical gap.

As a final issue, the validity of the Beer law for these materials[19] is addressed. Beer law can be written as[20]

$$\Delta OD = \epsilon \frac{\Delta Q}{zF} \quad [1]$$

where $\Delta OD$ is the optical density change, $\epsilon$ is the molar absorption coefficient, $\Delta Q$ is the inserted charge density, $z$ is the number of electrons transferred in the reaction, and $F$ is the Faraday constant. For anodic or cathodic coloring materials, a linear relationship between the optical density change and the inserted charge density is expected. The slope of the plot is defined as the electrochromic efficiency $\eta = \epsilon/zF$, quoted above. As a consequence of the ambiguous electrochromic behavior showed by the vanadium oxide thin films upon lithium insertion, it is important to define a direction for the electrochromic efficiency. For cathodic coloring materials, in which the optical density grows with the inserted charge, a positive $\eta$ value is assumed; in accordance, a negative $\eta$ value is assumed for anodically coloring materials. The time derivative of eq 1 can be written as

$$\frac{d(\Delta OD)}{dt} = \eta \frac{d(\Delta Q)}{dt} = \eta j \quad [2]$$

where $j$ is the current density. The validity of Beer's law for the sputtered vanadium oxide thin films implied a linear relationship between the current and the time derivative of the optical density change during the potentiodynamic experiments. In simpler words, a $d(\Delta OD)/dt$ vs $E$ plot should reproduce the potentiodynamic $j$ vs $E$ plot.

The comparison is shown in Fig. 8. Cathodic and anodic current peak positions and relative intensities shown in the potentiodynamic plot are reproduced in the $d(\Delta OD)/dt$ vs $E$ plot. Such an agreement clearly indicates the validity of Beer's law for the vanadium oxide films upon lithium insertion and deintercalation, once the sign of the electrochromic efficiency is taken into account.

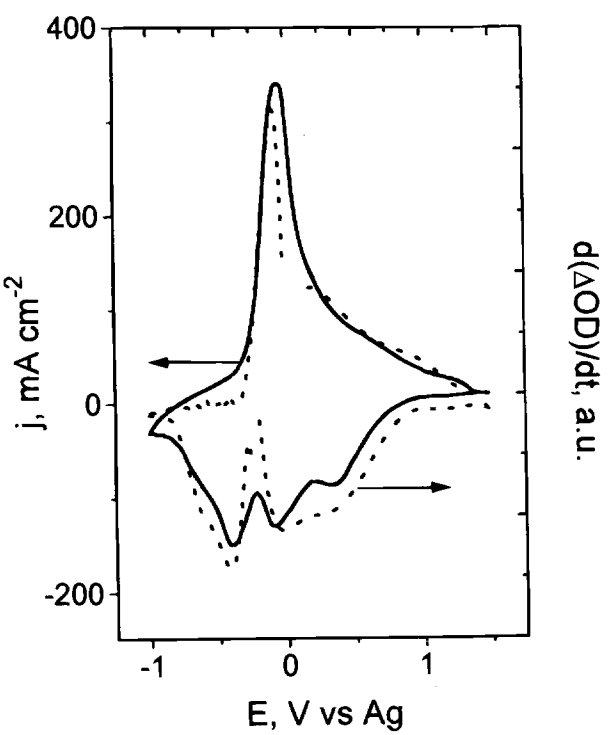


**Fig. 8. Potentiodynamic and time derivative of the optical density change plots for a thin film sample deposited with $\phi$ = 1.5 sccm. Scan rate: 5 mV/s.**

## Conclusions

In this work, vanadium oxide films deposited by rf reactive sputtering at different oxygen flows during deposition were characterized. The films were mostly amorphous or with a nanocrystalline structure. Films deposited at high $\phi$ had the $V_2O_5$ stoichiometry; films deposited at low $\phi$ contained a mixture of high and low oxidation state vanadium oxides. All samples contained hydrogen probably bonded to oxygen to form O-H groups and water molecules.

The vanadium oxide films deposited at the lowest $\phi$ did not show electrochromic activity in spite of their ability to intercalate substantial amounts of lithium. Such a characteristic makes them promising for application as electrochemically passive electrodes in electrochromic devices.

The films deposited at high $\phi$ were electrochromic with a maximum transmittance change of about 35%. Upon lithium intercalation, they showed a double electrochromic behavior depending on the wavelength and the intercalation extent. The electrochromic efficiency $|\eta|$ is about 8 $cm^2/C$ at $\lambda$ = 632.8 nm, either for the cathodically and the anodically coloring regions of intercalation level.

In agreement with other authors, a blue shift of the optical gap was observed for the electrochromic films. Furthermore, the validity of Beer's law for such films has been experimentally verified.

## Acknowledgments

Fapesp and CNPq provided financial support for this work. We acknowledge F. D. Origo for the spectrophotometer measurements.

Manuscript submitted February 4, 1997; revised manuscript received August 14, 1997. This was Paper 664 presented at the San Antonio, TX, Meeting of the Society, October 6-11, 1996.

*The Instituto de Fisica da Universidade de São Paulo assisted in meeting the publication costs of this article.*

REFERENCES

1. C. G. Granqvist, *Handbook of Inorganic Electrochromic Materials*, Elsevier Science, Amsterdam (1995).
2. A. Gorenstein, F. Decker, M. Fantini, and W. Estrada, in *Large-Area Chromogenic Materials and Devices for Transmittance Control*, Vol. I S4, p 272, SPIE Optical Engineering Press (1990).
3. S. I. Cordoba de Torresi, A. Gorenstein, R. M. Torresi, and M. V. Vazquez, *J. Electroan. Chem.*, **318**, 131 (1991).
4. S. Passerini, A. L. Tipton, and W. H. Smyrl, *Sol. Energy Mater. Sol. Cells*, **39**, 167 (1995).
5. A. Talledo and C. G. Granqvist, *J. Appl. Phys.*, **77**, 4655 (1995).
6. A. M. Andersson, A. Talledo, C. G. Granqvist, and J. R. Stevens, in *Electrochromic Materials*, M. K. Carpenter and D. A. Corrigan, Editors, PV 90-2, p 201, The Electrochemical Society Proceedings Series, Pennington, NJ (1990).
7. C. Julien and G. A. Nazri, *Solid-State Batteries*, Kluver Academic Pub., Boston, MA (1994).
8. C. R. Aita and M. L. Kao, *J. Vac. Sci. Technol.*, **A5**, 2714 (1987).
9. C. R. Aita, L. J. Liou, C. K. Kwok, R. C. Lee, and E. Kolawa, *Thin Solid Films*, **193/194**, 18 (1990).
10. J. Luksich and C. R. Aita, *J. Vac. Sci. Technol.*, **A9**, 542 (1991).
11. J. Tauc, in *The Optical Properties of Solids*, F. Abeles, Editor, North Holland, Amsterdam (1972).
12. M. Benmoussa, E. Ibnouelghazi, A. Bennouna, and E. L. Ameziane, *Thin Solid Films*, **265**, 22 (1995).
13. E. Cazzanelli, G. Mariotto, S. Passerini, W. H. Smyrl, and A. Gorenstein, *Solar Energy Mater. Solar Cells*, Submitted.
14. I. C. Faria, M. Kleinke, A. Gorenstein, M. C. A. Fantini, M. Tabacnicks, and C. Salvadori, in *Electrochromic Materials III*, K. C. Ho, C. B. Greenberg, and D. M. MacArthur, Editors, PV 96-24, p 79, The Electrochemical Society Proceedings Series, Pennington, NJ (1996).
15. C. Cartier, A. Tranchant, M. Verdaguer, R. Messina, and H. Dexpert, *Electrochim. Acta*, **35**, 889 (1990).

16. N. Kumagai, K. Taiino, T. Nakajima, and N. Watanabe, *ibid.*, **28**, 17 (1983).
17. W. R. Mckinnon and R. R. Haering, *Modern Aspects of Electrochemisty*, Vol. 15, p 235, Plenum Press, New York (1983).
18. J. Scarminio, A. Talledo, A. Andersson, S. Passerini, and B. Scrosati, *Electrochim. Acta*, 1637 (1993).
19. S. F. Cogan, in *Large-Area Chromogenics: Materials and Devices for Transmittance Control*, Vol. IS4, p 313, SPIE Optical Engineering Press (1990).
20. M. P. Cantão, I. J. Cisneros, and R. M. Torresi, *Thin Solid Films*, **259**, 70 (1995).

# Enhancement in Chemical Interaction at Conducting Polymers/n-Si Interfaces by Their Electroreduction

**Katsuyoshi Hoshino, Kentaro Tokutomi, Yoshiki Iwata, and Hiroshi Kokado**

*Department of Image Science, Faculty of Engineering, Chiba University, 1-33 Yayoi-cho, Inage-ku, Chiba 263, Japan*

ABSTRACT

Studies of chemical and electronic interaction at organic/inorganic interfaces are described. Electrochemical deposition of conducting polymers [poly(3-methylthiophene), polythiophene, poly(3-methylpyrrole), polypyrrole, poly(3-methylthiophene-co-pyrrole)] on an n-Si wafer does not give rise to high-quality p-n heterojunctions, but it is found that their junction properties are greatly improved by their electrochemical reduction (cathodic treatment). For example, the cathodic treatment of an as-grown poly(3-methylthiophene)/n-Si junction cell with rectifying ratio, $\gamma$, of $1.4 \times 10^1$ and diode factor, $n$, of 2.6 gives a high quality junction with $\gamma = 1.7 \times 10^4$ and $n = 1.2$. The treatment involves not only the development of polymer films but the improvement in junction interface, since the treatment can contribute to the improvement only when conducted in the presence of polymer films. In order to understand this modification at the interface, the effects of cathodic treatment conditions (treatment potential and time) and the presence of an interfacial oxide layer on the junction properties are investigated. As a result, it is revealed that the improvement is explained by a junction formation model described as the evolution of covalent bond formation at the interface. Further electrochemical studies reveal that such bondings are disrupted by hydrolysis and/or oxidation, and the bond disruption model is used to describe the degradation of the junctions in the air.

## Introduction

Current-controlled type organic thin film devices such as electroluminescent devices[1] have been attracting considerable attention in recent years, and a great deal of effort has been made in the design of device structure and material screening. However, there has been little analysis concerning electrode/organic film interface which may be one of the interfaces governing electrical properties of the devices. The understanding of organic film/electrode (in most cases, metal electrodes of thin film form) interface and some approaches for promoting the electronic interaction between the two phases are required for the attainment of highly efficient carrier injection into organic layers.

Egusa[2] investigated current injection from metal electrodes to organic layers (hole and electron transporting layers) and found that measured injection currents were three to six orders of magnitude lower than theoretical ones. Such a low current efficiency was explained by assuming that the density of states of organic materials is significantly lower than that of metals and/or that chemical bond formation between the two layers is scarcely expected to occur.

Metal/polymer interfaces have been studied by X-ray photoelectron spectroscopy, high-resolution electron energy loss spectroscopy, and infrared spectroscopy. Recent experiments revealed that C=O and aromatic sites on a polymer surface interacted with Al, Cu, Ti, and Cr metals, and metal-polymer complexes such as metal-O-C and metal-C were formed depending on metal and polymer materials.[3-5]

Chemical bond formation at an organic/inorganic interface and its effect on the junction properties are still somewhat controversial.[6,7] In order for organic films to offer viable alternatives to inorganics, intimate interaction between the two layers is required since highly efficient electron exchange between the layers and long-term stability of inorganic junction devices are based on the interaction. For the past several years, we have investigated junction properties of a p-type conducting polymer/n-Si contact as a model for inorganic/organic junctions. Current-voltage characteristics of this contact were sensitive to junction states at the interface, so that quantitative analyses of the interactions were made possible in terms of rectifying ratio ($\gamma$) and diode quality factor ($n$). Our previous studies pointed out

1. A high quality junction cannot be obtained simply by electrochemical deposition of a conducting polymer on an n-Si substrate. This is probably because active sites where the polymer is bonded covalently with the n-Si surface are small in number, and the thermal equilibrium of carriers, which is the basis of the formation of electrical double layer, is not fully established.[8]
2. The rectifying behavior is improved by employing sandblasted n-Si as a substrate. Fourier transform (FTIR) and potentiometric measurements showed that the number of bonds formed at the interface was enhanced by sandblasting the silicon substrate.[9]
3. A great improvement in junction properties is possible by treating the junction with an aqueous HF solution. Such high quality junction formation is described as the enhancement in interactions between the two phases, i.e., the evolution of covalent bond formation at the interface.[10]

Here we report our finding that electroreduction (cathodic treatment) of conducting polymers/n-Si junctions causes greater improvement in junction characteristics compared with the sandblasting and the HF treatment. The optimum electrochemical conditions of the cathodic treatment is determined, and a mechanism is suggested to account for the formation of high-quality heterojunctions.

## Experimental

Heterojunction cells were prepared on (100)-oriented n-Si wafers (resistivity: 0.001 ~ 0.015 Ω cm, dopant: Sb, obtained from ShinEtsu Co.) by electrochemical polymerization of monomers using a potentiostat/galvanostat (Hokuto Denko Company, model HA-301). The monomers used were 3-methylthiophene (3MeT, >99%), thiophene (T, >98%), 3-methylpyrrole (3MePy), and pyrrole (Py, >99%) from Tokyo Kasei Company, and were purified by distillation just before their use. The films of poly(3-methylthiophene) (P3MeT), polythiophene (PT), poly(3-methylpyrrole) (P3MePy), and polypyrrole (PPy) were deposited